

# Analysis of Throughput and Pathloss in 5g Wireless Communication Under MIMO Channel Environment

P. Parameswari<sup>1</sup>, G.K. Gobikaa<sup>2</sup>, S. Priyanka<sup>3</sup>, R. Arasakumar<sup>4</sup>,  
<sup>1,2,3,4</sup> Velammal college of engineering and Technology  
<sup>1,2,3</sup> B.E final year <sup>4</sup> Assistant Professor

**Abstract** - In this paper Terahertz (THz) band line-of-sight  $2 \times 2$  multiple-input multiple-output (MIMO)-sparse code multiple access (SCMA) systems is proposed to enhance the system performance. This proposed method is based on a sub harmonic mixer and translates the measuring frequency of vector network analyzer in the range of 298–313 GHz. The system employs a virtual antenna array method to distinguish a MIMO channel. The antenna factor spacing is derivative from the principles of diffraction inadequate optics to start parallel channels for higher system throughput and consistency. we build a joint sparse diagram combining the particular graph of MIMO channels and SCMA code words, and then propose the matching virtual SCMA codebooks for the detector. Furthermore, two strategies for message update on the joint sparse graph, i.e., parallel and serial schedules, are, correspondingly, offered. The MIMO channel measurements are finally used to estimate the performance of the communication system operating in THz band MIMO communication channel. Furthermore, we have shown the MIMO link in THz band operating at 7 Gb/s, with higher reliability.

**Index Terms**— *Index Terms*—Antenna arrays, channel sounding, indoor propagation measurements, MIMO systems, SCMA, MIMO, joint sparse graph, MPA.spatial diversity, THz channel propagation measurements, THz communication, THz system.

## I. INTRODUCTION

AS the requirement of efficient and reliable wireless communications with terahertz band (0.3 – 10 THZ) and high throughput are improving in fifth generation (5G) wireless communication. Terahertz Band (0.3 - 10 THz) communication is magnetizing more significance due to its large available bandwidth, small antenna size and high directivity. Since the large bandwidth is essential in allowing very high speed communication that is envisioned in future generation of wireless communication. In our existing wireless technology need higher data rates, where the MIMO techniques should be included in the THz Band wireless communication. This technique is potentially increasing the data rates and improving reliability of the systems. MIMO communication links give higher data throughput without increasing the system bandwidth. Multiple closely spaced transmitters (TX) and receivers (RX) are designed to launch parallel communication channels that can concurrently enhance the throughput and reliability of the system. Sparse code multiple access (SCMA) is a codebook-based non-orthogonal access technology, which is extensively considered as one promising applicant to support huge

connectivity and increase system capacity of next generation wireless communication systems. In addition, multiple-input multiple-output (MIMO) has also been designed for key enabling technology to enhance spectral efficiency by using spatial multiplexing. MIMO in conventional low frequency communication systems (2 - 5 GHz) uses multipath signals in a non-line-of-sight (NLOS) channel to achieve spatial diversity. However, in THz Band communication, LOS MIMO is more suitable due to small antenna size and high directivity. Even though high directivity is more flat to link breakage caused by path obstructions, a large array of MIMO links can easily mitigate this shortcoming. To characterize THz Band radio channel, several channel sounders and measurements have been reported. A 300 GHz measurement system is illustrated by single transmitter receiver with 9 GHz bandwidth in . channel response of single-input single-output (SISO) at 300 GHz is exposed using sub harmonic schottky diode mixer and a VNA. LOS and NLOS measurements at 300 GHz are performed with a system bandwidth of 20 GHz .However, to date, no MIMO link operating in THz Band has been investigated. To estimate a MIMO channel operating in THz Band, we have followed a  $2 \times 2$  MIMO system using linearly transferring a single transmit and receive antenna to form a virtual antenna array . The millimeter wave band from 60-95 GHz presents large swathes of unlicensed and semi-licensed spectrum between the transmitter and receiver, in which the measured MIMO channel matrix is then used in a communication system simulation to estimate the channel performance. To further progress the spectral efficiency, SCMA can be combined with MIMO technique. In which the existing researches mostly focus on the capacity examination. Really, how to improve the transmitted data bits between multiple users is also the vital problem of MIMO-SCMA systems and require to be solved. The optimal maximum likelihood (ML) detector is usually prohibitively complex for use in practical scenarios. So, for MIMO-SCMA systems, designing a low-complexity detector to accomplish near-optimum BER performance is a challenge.

In this paper, we present a novel joint SCMA and THz Band LOS MIMO detector can be used to evaluate the channel performance. The higher path loss and antenna directivity be able to enhance frequency reuse as well as multiply capacity of the THz Band system when deployed in a femto cell regime. Experimentally, we combine the joint sparse graph with single graph of MIMO and SCMA, and design the equivalent virtual SCMA codebooks. Finally,

based on them, MPA is directly applied to reconstitute the transmitted data bits. To the greatest of our knowledge, this is the first work investigating the mutual detection of SCMA and MIMO on a whole sparse graph. Simulations demonstrate that the proposed detector can accomplish a near-optimum BER performance with extensively reduced complexity. The remainder of this letter is structured as follows. In Section II, we describe our THz Band MIMO measurement system and channel response. In Section III, we show the performance of our emulated MIMO link. Finally, we conclude the letter in Section IV.

## II. THZ BAND MIMO MEASUREMENT SYSTEM

### A. Channel Measurements Testbed Specifications

The setup used for MIMO channel measurements consists of two major parts, Anritsu Vector Network Analyzer (VNA) MS4647B and VDi WR2.8MixAMC modules. VNA MS4647B is wideband equipment with the upper frequency limit of 70 GHz. To extend the frequency of the system to 300 GHz, WR2.8MixAMC are attached with the VNA. These extension modules are based on sub harmonic mixers that upconvert and downconvert the RF signal of the VNA. Detailed description of the setup is given. The block diagram of our setup is shown in Fig. 1. Yttrium iron garnet (YIG) based synthesizer was used to generate a common local oscillator signal  $f_{LO}$  of 12.357 GHz for both the upconverter and downconverter modules to achieve phase coherence. WR2.8MixAMC module multiplies this  $f_{LO}$  signal 24 times to generate THz Band signal, which is fed to  $f_{LOTHz}$  port of subharmonic mixer. Intermediate frequency  $f_{IF}$  port of this mixer is attached to the VNA that generates a sweep signal from 1 - 15 GHz. After mixing, the signal generated at the output of the subharmonic mixer contains frequencies from 298 - 313 GHz ( $f_{LOTHz} + f_{IF}$ ). This signal undergoes attenuation and phase alteration as it passes through the wireless channel. The signal is received at the receiver and fed back to the VNA after down conversion. The VNA determines changes in the received signal based on the information of transmitted signal and calibration data to show scattering parameters (s-parameters) of the channel. For measuring channel response, through/reciprocal calibration is performed with direct interconnection of the module's waveguide. All the later measurements are recorded with horn antenna attached at the output and input port of the transmitter and receiver, respectively. Antenna gain is 25 dBi each, with 3 dB beam width of  $12^\circ$ .

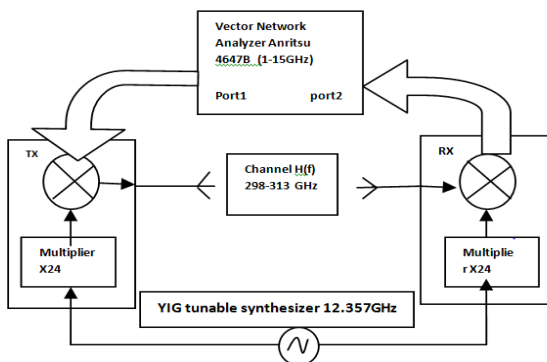


Fig. 1. Block diagram of THz Band measurement setup.

### b. Joint Sparse Graph-Detector Design

For downlink MIMO-SCMA detector, the output of MIMO detection cannot be effectively as the input of SCMA detection, as the spatial streams (orthogonal resources) only by hard-decision detected for MIMO can be used for the MPAbased detection of SCMA. To tackle this problem and reduce the detection complexity, we attempt to design a novel joint MPA-based detector to accomplish the combined detection of MIMO and SCMA.

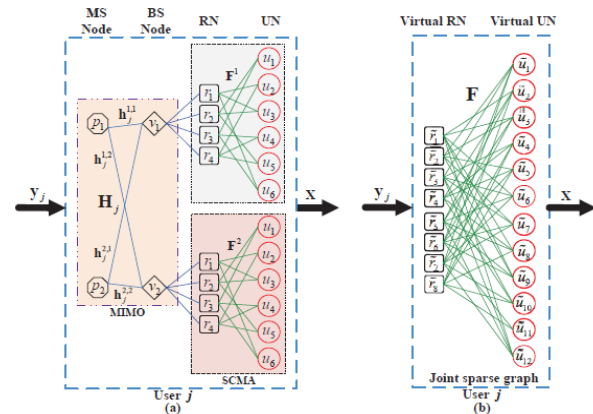


Fig. 2. The MIMO-SCMA receiver ( $J = 6, K = 4, N_B = 2, N_M = 2$ ). (a) Illustration of the original sparse graph; (b) Illustration of the joint sparse graph.1

As for the receiver in Fig. 2 (a), there are four types of nodes: MS nodes  $p_{nm}$  ( $n_M \in [1, N_M]$ ), BS nodes  $U_{nB}$  ( $n_B \in [1, N_B]$ ), resource nodes (RNs)  $r_k$  ( $k \in [1, k]$ ) and user nodes (UNs)  $u_j$  ( $j \in [1, J]$ ), representing the  $n_M$ -receive antenna, the  $n_B$ -transmit antenna, the  $k$ -th orthogonal resource and the  $j$ -user, respectively. A single graph, as labelled with SCMA in receiver, represents the low density signature due to SCMA structure. The other single graph, as labelled with MIMO in the receiver, represents the MIMO channel matrix. Due to the sparse feature of the SCMA codeword, the MIMO channel matrix  $H_j$  is also sparse. Note that, the factor graph of SCMA represents the relationship between RNs (e.g., subcarriers) and UNs, defined as  $F^{nB} = (f_1^{nB}, f_2^{nB}, \dots, f_j^{nB})$ . Thus, the sparse feature of  $X_j^{nB}$  can be expressed by the indicator vector  $f_j^{nB} \in \{0, 1\}^k$  where  $f_{k,j}^{nB} = 1$  indicates  $j$ -th user utilizes resource node  $k$ .

It can be seen from Fig. 2(a) that, BS nodes and RNs have the intermediary feature, as they are used to connect MS nodes and UNs through the sparse edges. In our proposal, we attempt to formulate an integrated sparse graph over which MIMO and SCMA detection can be performed in "one shot". Inspired by the observation of the sparsity of MIMO channel matrix and SCMA code words, the intermediary feature of BS nodes and RNs can be eliminated, and the factor graphs of the MIMO channels and the SCMA code words can be linked together, namely joint sparse graph for MIMO-SCMA, which is shown in Fig. 2(b). Based on the joint sparse graph model, we can utilize the MPA to perform MIMO and SCMA detection at the same time on the entire sparse graph. Now, we propose a two-stage processing structure consisting of

preprocessing (joint sparse graph construction) and post processing (MPA-based detection) for receiver.

*C. MIMO Measurements Based on Diffraction Limited Optics*

Unlike conventional low frequency MIMO that depends on NLOS multipath signals, THz Band MIMO is more appropriate with LOS spatial diversity scheme. This is because in THz Band, the high path loss causes the multipath signals to get very attenuated. On the other hand, the peculiar behavior of small antenna size makes LOS MIMO more promising technique as large number of antenna elements can be placed alongside a small area to make multiple parallel channels. The high directivity will make sure that the inter channel interference, generated due to closely placed transmitters, is minimal. The concept of THz Band  $N \times N$  LOS MIMO is shown in Fig. 3. In THz Band LOS MIMO, antenna separation  $D$  is a very important parameter ensuring multiple transmitters can be distinguished at the receiver. This problem is addressed by using diffraction limited optics theory, which states that for LOS MIMO, the antenna element spacing should be kept as

$$D = \sqrt{\frac{R \cdot \lambda}{N}}$$

where  $R$  is the distance between transmitter and receiver,  $\lambda$  is the free space wavelength of the carrier frequency and  $N$  is the number of elements at the receiver. This condition is very similar to Rayleigh criterion. It is evident that there will be cross channel interference among different channels; this interference can degrade the performance and must be reduced using a channel separation network, as shown in Fig. 4.

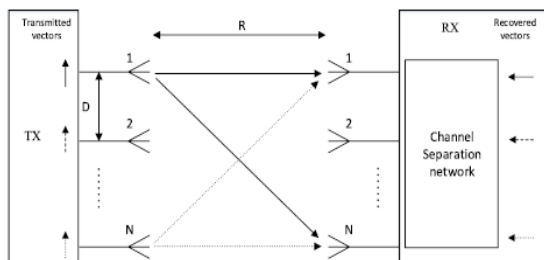


Fig. 3. Block diagram of THz Band measurement setup.

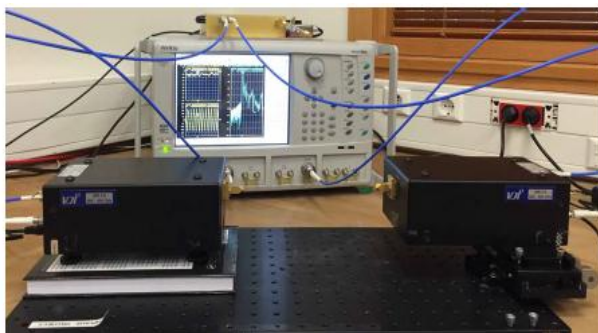


Fig. 4. THz Band  $N \times N$  LOS MIMO system(Existing model)

Measurements were conducted in NWCL lab, which is a typical single floor office environment. The setup for  $2 \times 2$  LOS MIMO channel experimentation was placed on a solid aluminum optical breadboard with matte anodized finish that reduces unwanted reflection. Distance between the transmitter and the receiver was kept as  $R = 25$  cm. For such small distance and narrow antenna beam width along with high path loss, reflected NLOS signals can be neglected. At a center frequency of 305.5 GHz, the corresponding inter element spacing calculated using (1) is  $D = 1.2$  cm. On the other hand, VNA was configured to record full 14 GHz band measurements with 1 KHz intermediate frequency bandwidth (IFBW). Details of the measurement parameters are given in Table I and our measurement setup is shown in Fig. 5. To acquire a full  $2 \times 2$  LOS MIMO channel matrix, we first recorded the response of MIMO TX 1 in both the channels. This was carried out by placing transmitter module at antenna location 1 of the TX and the receiver module at antenna

TABLE I  
MEASUREMENT PARAMETERS OF VNA

Parameter	Symbol	value
Measurement points	N	7368
Test signal power	$P_{in}$	-10 dBm
Start frequency	$f_{start}$	1 GHz
Stop frequency	$f_{stop}$	15 GHz
Bandwidth	B.W.	14 GHz
IFBW	$\Delta f_{IF}$	1 KHz

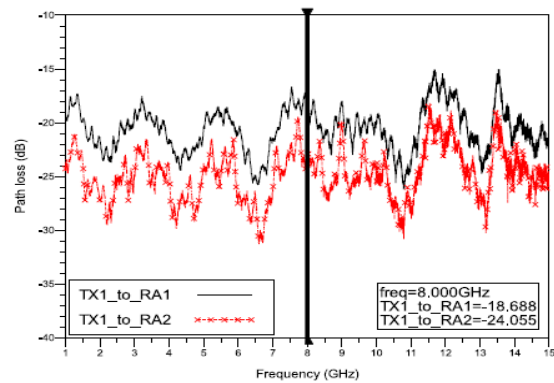


Fig. 5. Signal magnitude of TX 1 at RA 1 and cross channel interference magnitude at RA 2.

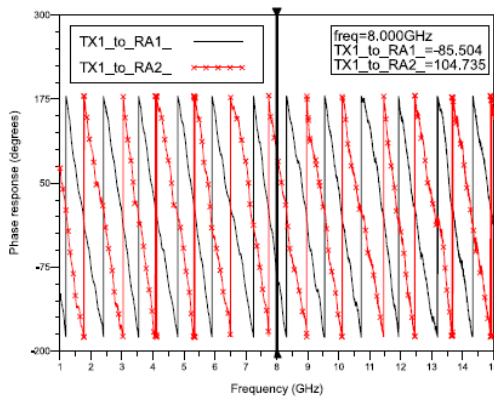


Fig. 6. Signal phase of TX 1 at RA 1 and cross channel interference phase at RA 2.

location 1 (RA1) of RX. The receiver module was then displaced to antenna location 2 (RA2) of RX. In our setup, the desired phase response was obtained at 1.257 cm away from the previous position, which agrees with our theoretical estimate based on (1). The first configuration measures the response of signal transmission in channel 1 (CH1) and the second configuration measures cross channel interference in channel 2 (CH2) due to MIMO TX 1.

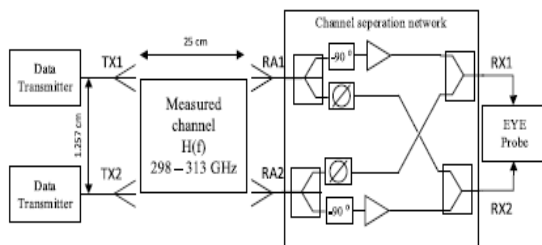


Fig. 7. Schematic of 2 × 2 THz Band MIMO system.

The downconverted magnitude response is shown in Fig. 4 and phase response in Fig. 6. It can be seen in Fig. 5 that the phase difference of the received signal at adjacent antennas is 180°. Similarly, frequency response of MIMO TX 2 was recorded at both RX antenna locations to create a virtual array. The recorded measurements were combined to generate a full 2 × 2 channel matrix. This matrix was used to perform post processing on a computer to evaluate the performance of THz Band 2 × 2 MIMO channel. The cross channel signal at any receiver is out of phase and can be suppressed using a channel separation network. This network mainly consists of delay elements, amplifiers, and splitter/combiner. The architecture of channel separation network is shown in Fig. 7. The optimal values of the amplifier and phase delay element were iteratively determined while minimizing cross channel interference. In CH1, the corresponding optimal value for amplifier gain was found as 7.24 dB and the phase delay was 85.19° whereas, in CH2, the amplifier gain was 7.69 and the phase delay was 84.58°.

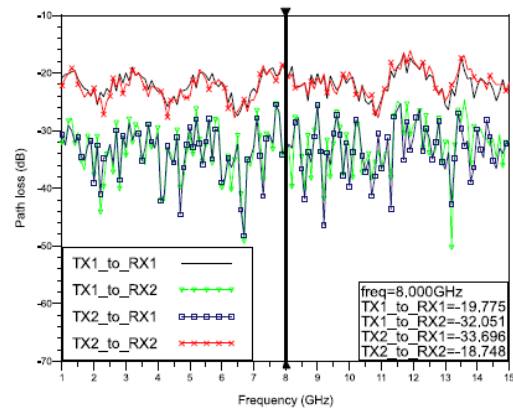


Fig. 8. Path loss of CH1 (TX1\_to\_RX1) and CH2 (TX2\_to\_RX2) along with cross channel interference magnitude at receiver 1 (TX2\_to\_RX1) and receiver 2 (TX1\_to\_RX2), after channel separation network.

The slight difference in these component parameters is due to the fact that the response for both channels was not exactly identical in an office environment. Signal magnitude after channel separation network is shown in Fig. 8. It can be seen that the cross channel interference is 13.9 dB below the main signal magnitude and is much higher than the noise level, which is -40 dB. Hence the throughput will be determined by the signal to interference ratio. However, for distances greater than 50 cm, the noise will dominate and hence the throughput will be chiefly determined by the signal to noise ratio (SNR).

### III. SIMULATION RESULTS AND DISCUSSIONS

In this section, the performance of MIMO-SCMA systems is evaluated by comparing the proposed detector with the existing techniques. Computer simulations are carried out over Rayleigh flat fading channels. Without loss of generality here we assume that each user adopts the same codebook for different transmit antennas, i. e.,  $x_j^{nB} = x_j$ . The user-specific codebooks are designed. Fig.9, signal magnitude of Tx1 and Tx2 and cross channel interference magnitude at RX2. As comparing with existing method, here noise level is reduced. We analyse that maximum noise level is 4.5 dB.

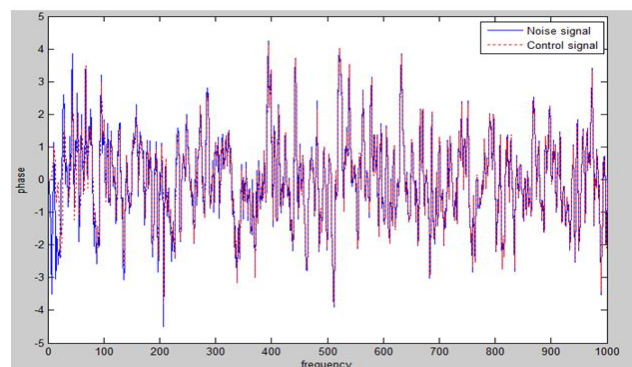


Fig.9 signal magnitude of TX1 and RX1 with cross channel interference magnitude of RX2

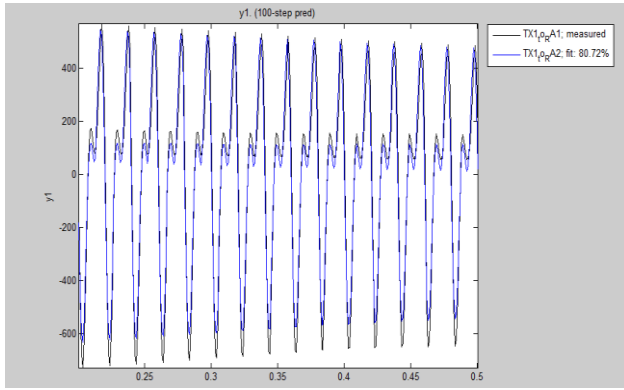


Fig.10,Signal phase of TX1 and RX1,TX1 and RX2

Next we measure the signal phase between transmitter1 and receiver 1, transmitter1 and receiver2(cross channel interference), value of the phase set to 400 to -400.Resultant output for signal phase is shown in fig.9.

Pathloss of each channel (TX1 to RX1,TX1 to RX2,TX2 to RX1,TX2 to RX2) along with cross channel is determined.Most of the losses occur in the negative level while comparing with existing model here loss is reduced.Thus fig.11a shows the pathloss of channel1(TX1-RX1) and channel2(TX2-RX1) alongwith cross channel interference for path1.Fig.11b shows pathloss of channel1(TX1-RX1) and channel2(TX1-RX2) alongwith cross channel interference for path 1.Fig.11c shows shows pathloss of channel1(TX1-RX2) and channel2(TX2-RX2) alongwith cross channel interference for path 1.

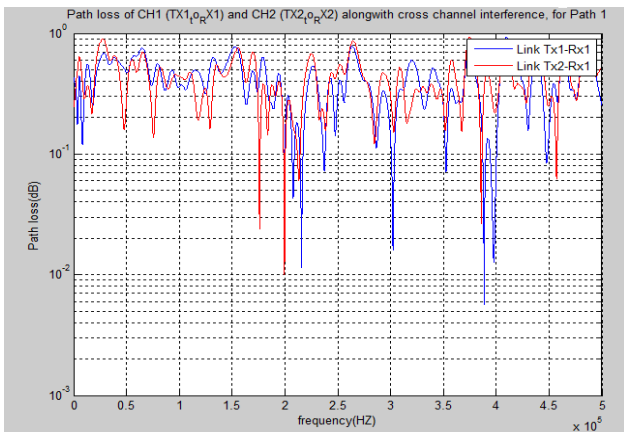


Fig.11a

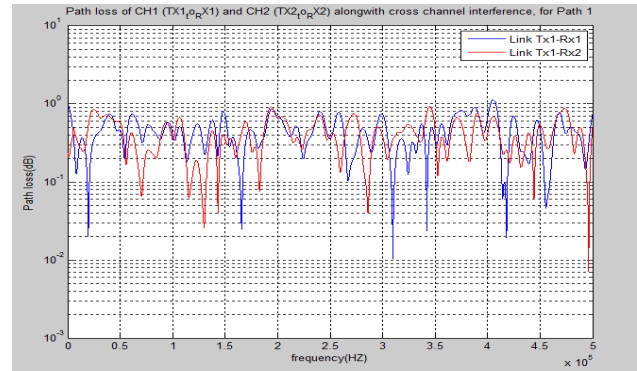


Fig.11b

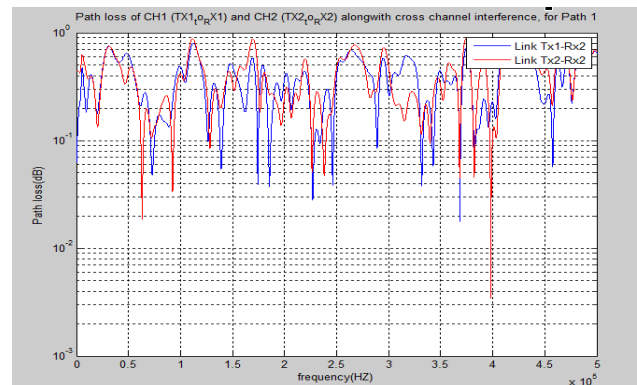


Fig.11c

For reducing the noise level only,code is generated with the sub harmonic algorithm along with SCMA.The transmitter generates pseudorandom binary sequences, the measured MIMO channel response, a channel separation network and an equalizer.Distance between two channel is kept as 0.5cm. The system was analyzed for different configurations such as single transmit mode, MIMO CH1 and MIMO CH2. While operating in single transmit mode, other channel was kept silent, whereas, in MIMO channel configuration, other channel was excited by uncorrelated bits to imitate cross talk scenario.

#### IV. CONCLUSION

We have presented THz Band  $2 \times 2$  LOS MIMO system operating at 7 Gbps. Spatial diversity scheme is utilized with antenna element spacing derived from the principles of diffraction limited optics. The channel transmission and inter channel interference is measured and recorded using virtual antenna array technique and channel sounder based on VNA and frequency extenders. A joint sparse graph detecting is proposed to approach the BER performance of the ML detector with reduced complexity for downlink MIMO-SCMA systems. To strike a balance between detector complexity and latency, two schedules, parallel and serial schedules, are presented. Simulation results show the superiority of proposed detector. We have shown that cross channel link vectors are out of phase and can be suppressed using channel separation network. Optimal channel separation parameters were determined for minimal cross channel interference. Finally, THz Band  $2 \times 2$  MIMO link was evaluated for digital communication system and

confirmed to achieve 7 Gbps. However, a significant difference was seen between the theoretical and experimental throughputs that opens up the need for further research. Moreover, our results suggest that single carrier might not provide the ultimate benefit of such a wireless communication channel, instead multi-carrier modulation will perform better in terms of spectral efficiency, given its relative immunity to fading and interference. Future works in this domain are to analyze systems with larger one-dimensional and two-dimensional arrays transmitting real time data in different indoor environments. Performance of multi-carrier modulation system may also be analyzed.

#### REFERENCES

- [1] L. L. Dai, B. C. Wang, Y. F. Yuan S. F. Han C. L. I and Z. C. Wang, "Nonorthogonal multiple access for 5G: solutions, challenges, opportunities, and future research trends," *IEEE Commun. Mag.*, vol. 53, no. 9, pp. 74-81, Sept. 2015.
- [2] H. Nikopour, H. Baligh, "Sparse code multiple access," in *IEEE PIMRC*, pp. 332-336, Nov. 2013.
- [3] F. Boccardi, R. W. Heath, A. Lozano, T. L. and P. Popovski, "Five disruptive technology directions for 5G," *IEEE Commun. Mag.*, vol. 52, no. 2, pp. 74-80, Sept. 2014.
- [4] S. Priebe *et al.*, "Channel and propagation measurements at 300 GHz," *IEEE Trans. Antennas Propag.*, vol. 59, no. 5, pp. 1688-1698, May 2011.
- [5] N. Khalid and O. B. Akan, "Wideband THz communication channel measurements for 5G indoor wireless networks," in *Proc. IEEE Int. Conf. Commun. (ICC)*, Kuala Lumpur, Malaysia, May 2016, pp. 1-6.
- [6] C. Gustafson, K. Haneda, S. Wyne, and F. Tufvesson, "On mm-wave multipath clustering and channel modeling," *IEEE Trans. Antennas Propag.*, vol. 62, no. 3, pp. 1445-1455, Mar. 2014.
- [7] E. Torkildson, B. Ananthasubramaniam, U. Madhow, and M. Rodwell, "Millimeter-wave MIMO: Wireless links at optical speeds," in *Proc. 44<sup>th</sup> Allerton Conf. Commun. Control Comput.*, Monticello, IL, USA, 2006, pp. 36-45.
- [8] C. Sheldon *et al.*, "A 60GHz line-of-sight 2x2 MIMO link operating at 1.2Gbps," in *Proc. IEEE Antennas Propag. Soc. Int. Symp. AP-S*, San Diego, CA, USA, Jul. 2008, pp. 1-4.
- [9] A. Sanders, M. Resso, and J. D'Ambrosia, "Channel compliance testing utilizing novel statistical eye methodology," presented at the DesignCon, Santa Clara, CA, USA, 2004, pp. 1-25.
- [10] Yang Du, Binhong Dong, Zhi Chen, "Joint Sparse Graph-Detector Design for Downlink MIMO-SCMA Systems" *IEEE Wireless Communications Letters*
- [11] Nabil Khalid, Ozgur B. Akan, "Experimental Throughput Analysis of Low-THz MIMO Communication Channel in 5G Wireless Networks", *IEEE Wireless Communications Letters*, VOL. 5, NO. 6, DECEMBER 2016.